
Predictive Model for ^{82}Rb Generator Bolus Times as a Function of Generator Lifetime

Alexander W. Scott¹, Mark Hyun¹, and Jennifer Kim²

¹Department of Imaging, Cedars-Sinai Medical Center, Los Angeles, California; and ²Department of Clinical Research Operations, City of Hope, Duarte, California

^{82}Rb cardiac PET is largely used to study myocardial perfusion with function and to calculate myocardial blood flow (MBF) and coronary flow reserve or myocardial flow reserve. Although the dosing activity of ^{82}Rb is determined by the patient weight, the infusion volume and activity concentration varies with the age of the ^{82}Rb generator. We sought to predict the needed bolus volume of ^{82}Rb to help evaluate the accuracy of MBF findings.

Methods: Data were collected from deidentified tickets of an ^{82}Rb generator, including the instantaneous eluted activity flow rate. The times to reach 4 activity levels—740, 1,110, 1,480, and 1,665 MBq (20, 30, 40, and 45 mCi, respectively)—were also calculated. The activity flow rate for the largest bolus was fitted to determine the functional form. The time to reach each bolus level was fitted as a function of the generator age, and 95% CIs were created. **Results:** The activity flow rate was fitted with a growth-saturation model, allowing a calculation of bolus volume. The amplitude of the fit was observed to also be influenced by the time since the last elution and possibly other clinical factors. Elution times to reach the 4 activity levels were plotted versus generator age. The linearized data were fitted, and 95% CIs were created symmetrically around the fit. The 95% CI band allowed a prediction of elution time to achieve each bolus size for future generators, as a function only of generator age. **Conclusion:** A predictive model was created for elution times from this brand of ^{82}Rb generator as a function of generator age. The value of this model is in determining whether the necessary amount of activity can be extracted from a generator before reaching one of the backup infusion settings, such as volume limits per administration, given a generator age. Some sites may also control the bolus duration for better MBF calculations, since predicting the time for the injection to complete may determine whether MBF and coronary flow reserve calculations are meaningful.

Key Words: ^{82}Rb ; modeling; physics

J Nucl Med Technol 2022; 50:38–42

DOI: 10.2967/jnmt.120.256917

Although both myocardial perfusion SPECT and PET imaging provide valuable information on the 3-dimensional distribution of radiotracers into myocardium, there are

several physical differences by which PET has a clear advantage over SPECT (1). PET has a high spatial and temporal resolution, reliable attenuation and scatter correction, short imaging protocols using short-lived positron-emitting radiotracers to acquire 3-dimensional acquisitions simultaneously (which offers tracer kinetic models to obtain absolute myocardial blood flow [MBF] measurements for rest and stress, where *coronary flow reserve* or *myocardial flow reserve* are terms interchangeable with *rest MBF* and *stress MBF*, respectively), and relative perfusion and function analysis as well. These important properties of myocardial perfusion PET imaging translate into high diagnostic accuracy, consistent high-quality images, low radiation exposure, short acquisition protocols, routine quantification of MBF, and strong prognostic power.

According to a position statement by the American Society of Nuclear Cardiology and the Society of Nuclear Medicine and Molecular Imaging (2), rest–stress PET myocardial perfusion imaging is a preferred test for patients with known or suspected coronary artery disease who meet appropriate criteria and are unable to exercise adequately. Rest–stress PET myocardial perfusion imaging is recommended for patients with suspected coronary artery disease who also meet one or more of the following criteria: patients with poor-quality, equivocal, or inconclusive results on prior stress imaging or results that are discordant with clinical or other diagnostic test results, including findings at coronary angiography; high-risk patients with advanced kidney disease, diabetes, or known disease in the left main coronary artery, multiple coronary arteries, or the proximal left anterior descending coronary artery; patients who have undergone heart transplantation; young patients with coronary artery disease; and patients who need MBF to assess microvascular function.

According to a joint position paper of the Society of Nuclear Medicine and Molecular Imaging Cardiovascular Council and the American Society of Nuclear Cardiology (3), under resting conditions, autoregulation of myocardial tissue perfusion occurs in response to local metabolic demands. Rest MBF has been shown to vary linearly according to the product of heart rate and systolic blood pressure (3,4). Interpretation of the stress MBF results together with coronary flow reserve (myocardial flow reserve) accounts for the confounding effects of resting hemodynamics (heart rate and systolic blood pressure). To ensure accurate estimates of

Received Dec. 29, 2020; revision accepted Aug. 11, 2021.
For correspondence or reprints, contact Alexander Scott (alexander.scott@cshs.org).
Published online Sep. 28, 2021.
COPYRIGHT © 2022 by the Society of Nuclear Medicine and Molecular Imaging.

MBF and coronary flow reserve (myocardial flow reserve), it is critical to verify that each dynamic series is acquired and analyzed correctly. Therefore, it is important to note that consistent tracer injection profiles improve the reproducibility of MBF measurements and to ensure adequate sampling of the complete arterial blood input function (3).

Assessment and correction of patient motion between the first-pass transit phase and the late-phase myocardial retention images are essential, as motion can otherwise introduce a large bias in the MBF estimates compared with the relative perfusion image findings. The peak height of blood pool time–activity curves at rest and stress should be comparable if similar radiotracer activities are injected. If there are substantial differences, extravasation or incomplete delivery of tracer may have occurred and may result in inaccurate MBF estimates. Because variations in the tracer injection profile can adversely affect MBF accuracy, blood pool time–activity curve should be visually examined for multiple peaks or broad peaks, which may suggest poor-quality injections due to poor-quality intravenous catheters, arm positioning, or other confounding factors from the patient’s physiology (3).

Another potential source of variability in radiotracer delivery is the ^{82}Rb generator itself. The current recommendation is to inject a weight-based activity level to minimize population radiation dose (or collective dose, due to the ^{82}Rb procedures) (5). The ability to deliver a large dose for a large body habitus may be compromised as the generator reaches the end of its lifetime, since the activity curve for the daughter isotope delivered from a generator must vary as the parent isotope decays. The peak height of the activity curve will vary depending on whether the activity is injected as a bolus (activity concentrated in time and location) or is injected continuously as the generator struggles to produce. A recent guide from the American Society of Nuclear Cardiology and the Society of Nuclear Medicine and Molecular Imaging on PET measurements of MBF (6) recommends the following to control the duration of a bolus for accurate MBF measurement: ensure a good, free-flowing forearm intravenous line (20-gauge or larger) for tracer administration; flush with saline immediately after the tracer administration to help clear the blood pool activity; review and compare the rest–stress time–activity curves on dynamic images as a quality control; apply motion correction on dynamic images as needed; follow the weight- or body mass index–based dosing consistently; and schedule obese patients for an earlier generator cycle to minimize administering the suboptimum tracer activity because of the volume limit. The last 2 points, regarding bolus duration and weight-based dosing, are dependent on generator performance.

For these reasons, it may be of interest to develop a method for calculating the bolus length for a patient given that patient’s weight and the age of the generator (defined as days after calibration). If the time to achieve a complete bolus injection exceeds a level set by the nuclear cardiologist, or would exceed the infusion cart’s infusion volume

limit setting, then the patient will not receive the diagnostic quality as ordered. The examination may need to be rescheduled for a time when the generator is fresher or when the next generator has been installed, or the clinical approach may need to be changed. This article provides a formula for this calculation, which is based on deidentified injection printouts for a CardioGen-82 (Bracco) ^{82}Rb generator covering its full clinical life.

MATERIALS AND METHODS

The data sample came from deidentified tickets (data output) produced by 3 CardioGen-82 generators. All 3 were calibrated for 3,700 MBq (100 mCi) and were in use for 1 mo each, for a total of 491 elutions. Each generator was retired from clinical use after 1 mo, following institutional policy. One generator was studied independently, and then all generator data were combined for an overall analysis. The following information was extracted from each ticket: date, time, total injected volume, total injected activity, and injected activity rate at each second during the injection. For each elution, the peak injected activity rate was recorded and a calculation was made of the injection duration in seconds to inject up to 4 different activity levels (740, 1,110, 1,480, and 1,665 MBq [20, 30, 40, and 45 mCi, respectively]).

Two separate datasets were created for the purpose of predicting generator behavior. The first dataset was the complete injected activity curve for each injection, for the purpose of predicting the required time to administer a certain amount of activity. The injected activity rate curve of one large bolus injection was fitted using Microsoft Excel to determine the functional form of the bolus over time, and this functional form was applied to the other elutions. Once the functional form was verified, the peak injected activity rate was used as a proxy for the amplitude of the fit when comparing the individual elutions.

The second dataset consisted of the time to reach 4 different injected activity level as a function of the age of the generator, in days since calibration. For each of the chosen activity levels, 95% CI bands were created by fitting the data in OriginPro (OriginLab Corp.) using an exponential growth function of the form $y(t) = y_0 + A \cdot \exp\left(\frac{t}{t_1}\right)$, where $y(t)$ is the time to achieve a certain bolus of activity given a generator age t , y_0 is the threshold time (the generator is being eluted but activity is not injected until a threshold of 37 MBq [1.0 mCi]/s), A is the amplitude (s), and t_1 is the growth constant. A 95% CI band was created symmetrically around the fit by shifting y_0 (the y intercept) by $\pm \Delta y$ to encompass 95% of the data between the shifted curves. The fit and 95% CI band allowed prediction of the time to achieve that bolus size for future generators as a function of generator age.

RESULTS

The plot of injected activity per second over time for a single large bolus was well fitted by a growth-saturation model of the form $y(t) = y_0 + A \cdot (t - t_0) \cdot \exp(-C \cdot (t - t_0))$, shown in Figure 1. The reduced χ^2 of the fit was 0.61 using an uncertainty of 5% on the activity from the injection cart’s dose calibrator. This model allowed calculation of the total injected activity at any time during the elution. However, the peak injected activity rate did not follow an exponential decay with the age of the generator but peaked

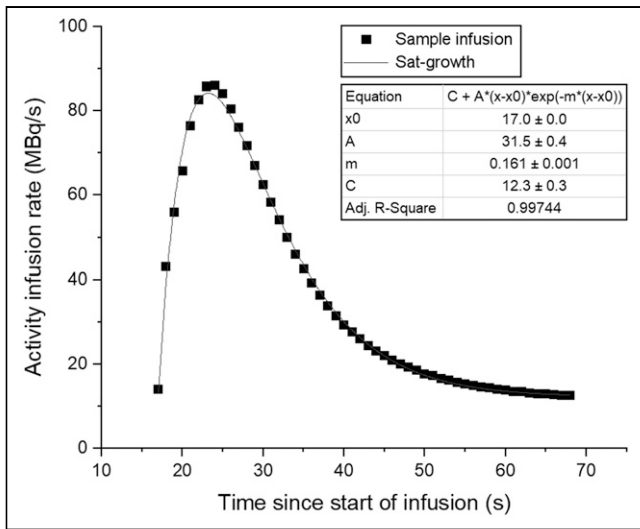


FIGURE 1. Activity infusion rate data and fit for sample bolus from February 9, 2017, with fit parameters for growth-saturation curve of form $y(t)=y_0+A \cdot (t-t_0) \cdot \exp(-C \cdot (t-t_0))$.

within a week of the calibration date of the generator. Also, the peak injected activity rate fluctuated throughout the day, as shown by the spread of peak injection activity rates in Figure 2.

The time to administer 4 different injected activity levels separated into distinct regions, although the bands that contained 95% of the data did overlap at low generator ages, as shown in Figure 3. The 740-MBq (20 mCi) activity level band contained results from 459 elutions, the 1,110-MBq (30 mCi) band contained results from 454 elutions, the 1,480-MBq (40 mCi) band contained results from 169 elutions, and the 1,665-MBq (45 mCi) band contained results from 60 elutions. The parameters of the best fit to the data,

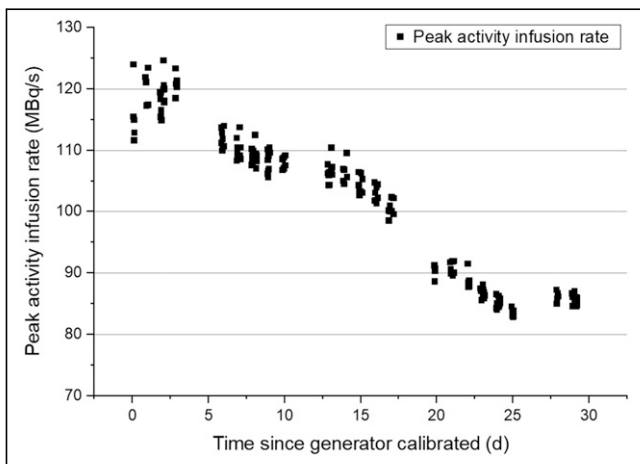


FIGURE 2. Peak activity infusion rate for each study from one representative generator as function of generator age. Amplitude of activity rate curve did not decrease exponentially with generator age as expected. There is also up to 10% variation in peak activity rates within a single day.

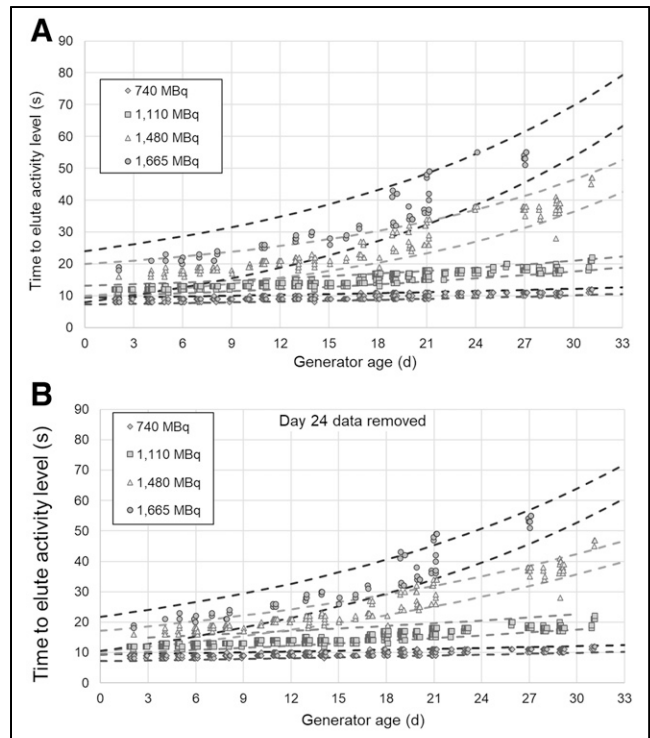


FIGURE 3. Best fit bands for 4 activity levels and time to elute each, as function of generator age. Each band contains 95% of data points for each injected activity level. Data are combined from 3 separate ^{82}Rb generators. Top image is with anomalous results from day 24; bottom image is without.

along with the Δy of the 95% CI bands, are listed in Table 1. These are the parameters of 4 exponential growth models (for the 4 target activity levels studied) of the form $y(t)=y_0+A \cdot \exp(t/t_1)$. Given the age of the generator, the user can calculate the duration of the bolus (s) that will produce one of the 4 activity levels described. Alternatively, the user can take an upper limit for the bolus duration and use the formula $t=t_1 \cdot \ln\left(\frac{y-y_0}{A}\right)$ to calculate the last day of generator life on which that bolus can (on average) be achieved.

Some data were excluded from this fit; data from the first 3 d of each generator, when the peak activity rate was increasing, were removed. Also, a single generator had data from 2 d that did not conform to the distribution of the other points, as evidenced by a large residual to the fit, and these data were removed.

DISCUSSION

Although the injected activity rate was well fitted, the amplitude did not depend solely on the physics of radioactive decay. The peak output activity rate (used as a proxy for the amplitude in the growth-saturation fit) increased for the first few days of use and then decreased throughout the week, except the rate did not decrease consistently over the weekend. The generator was not used over the weekend, but the data in Figure 2 for Fridays and Mondays do not

TABLE 1

Fit Parameters for Time to Elute Certain Activity Levels as Function of Generator Age, Following Functional Form

$$y(t) = y_0 + A \cdot \exp\left(\frac{t}{t_1}\right)$$

Fit (mCi)	y intercept (y_0) (s)	Amplitude (A) (s)	Growth constant (t_1) (d^{-1})	Band range (s)
20	6.05	2.31	37.54	± 1.05
30	6.25	5.21	32.60	± 1.70
40	9.25	5.70	17.33	± 5
45	2.93	13.12	20	± 8
Modified 45	16.22	3.15	10.96	± 2.5

Additional fit was performed for largest eluted activity (1,665 MBq) to demonstrate that data could be more precisely fitted without 2 days' worth of generator results.

show a consistent pattern. Following a similar pattern, a correlation between peak injection activity rate and length of time since the last elution was observed.

^{82}Sr and ^{82}Rb are in secular equilibrium, and a generator that is eluted every 10 min will have a daughter-to-parent ratio of 99.7%; because clinical practice dictates no less than 10 min between elutions, a correlation was unexpected. The correlation was determined using the Pearson method to produce a coefficient and correlation likelihood; for 1 generator, 100% of days with clinical use showed a 95% likelihood or greater correlation between the eluted peak activity rate and generator rest times. This positive correlation held true even to 350 min since the last elution, which is more than 2 orders of magnitude greater than the half-life of the ^{82}Rb daughter isotope. The variation in peak output due to time since the last elution (a maximum difference of 10%) is greater than the variation between days as the generator ages, as shown in Figure 4. Although longer rest times will have some marginal benefit to bolus lengths as

the generator ages, the variability of peak output with generator rest times is one of the confounding factors in presenting a completely deterministic model.

These 2 complications are consistent with findings from the initial development of the $^{82}\text{Sr}/^{82}\text{Rb}$ generator by TRIUMF (7). As the generator was eluted over time, the distribution of ^{82}Sr within the generator column changed from a narrow band at the top of the column to a much broader peak toward the bottom. Therefore, one would expect the diffusion rate to be higher later in the generator's life because of the greater surface area covered with ^{82}Sr . In a private communication with a Bracco scientist (Dr. Adrian Nunn, oral communication, February 20, 2018), it was confirmed that rest periods of longer than 10 min should result in greater activity in solution because chemical equilibrium has not yet been reached.

Regarding the fit to the second dataset, the prediction band for 1,665 MBq (45 mCi) had much less precision than the bands for other activity levels, having a bandwidth of 8 s compared with 1–2 s for 740- and 1,110-MBq (20 and 30 mCi) activity levels. Subtracting 1 d of data from each of 2 different generators reduced the bandwidth to 2.5 s while keeping 52 of the 60 data points. Although there is not a priori justification for this change to the dataset, it does suggest that the true distribution of bolus times is more narrow and that there is an uncontrolled variable causing longer elution times on certain days. One possibility is that the intravenous gauge used clinically was different for those 2 d, since the elution times were significantly longer given the eluted activity.

The clinical significance of the model was varied across different dose limits. The effect of the bolus lengthening can be best seen at 42 d, which is the generator expiry limit. For an elution of 740 MBq (20 mCi), the model

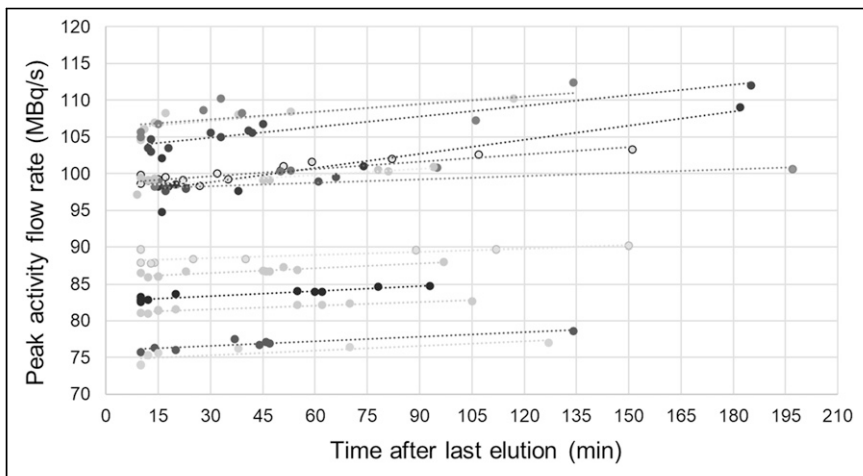


FIGURE 4. Peak activity injection rate for each elution, compared with time since last elution. Lines connect data from same day, such that points come from same generator age. Ten minutes is minimum spacing for clinical use, and no studies had time of less than this value since last elution. On the basis of secular equilibrium assumptions, $^{82}\text{Rb}/^{82}\text{Sr}$ ratio should be 99.7% of its maximum at 10 min. Elution continues to produce higher peak activity rates with resting times up to 3 h, the longest time measured.

predicts an elution time of 13 s at day 42, which is not much more than the 8.5 s predicted for day 2. Meanwhile, the 1,665-MBq (45 mCi) model predicts an elution time of 110 s at day 42, in contrast to the 17 s required on day 2.

Our institution limits the infusion to 50 mL to a patient, which although more restrictive than the prescribing information limit of 100 mL, may be more relevant to clinical practice. With a flow rate setting of 50 mL/min, and a start-up time of approximate 14 s, the maximum elution time is 74 s before triggering the elution to stop. For a cutoff time of 74 s, the model predicts that the last day to achieve 1,665 MBq (45 mCi) is day 34; the last day to achieve 1,480 MBq (40 mCi) is day 42. The other 2 activity levels, 740 and 1,110 MBq (20 and 30 mCi), will not be limited before the expiry of the generator.

CONCLUSION

We were able to develop predictions for the time to elute a bolus of certain durations from an ^{82}Rb generator as a function of generator age. Given the flow rate (mL/min) setting selected by the user, the volume of the bolus can be determined from the duration of the elution. Although the eluted activity rate over time was well fitted by a growth-saturation curve, the amplitude of this curve was not dependent just on generator age but also on factors such as generator rest times and likely clinical factors such as patient circulatory resistance and gauge of an intravenous line as well.

There were real instances of truncated elutions; within the datasets collected, there were a few elutions in which the full prescribed activity was not delivered because of triggering of the limit on patient volume (50 mL). For a 1,665-MBq (45 mCi) prescribed activity on day 31 of the generator, the elution was cut off at 72 s because the patient volume limit was hit, and the observed elution time is within the prediction range. The prediction bands for different activity levels allow for a range of bolus injection times that run up to 66 ± 8 s for 1,665 MBq (45 mCi) on day 31.

The consequences of performing a coronary flow reserve examination using a bolus duration of 61 s (1,665 MBq, or 45 mCi, on day 30) could include erroneous myocardial flow reserve calculations. The authors of this article reviewed our institution's records for patients with myocardial flow reserve calculations and whose examinations resulted from different ^{82}Rb generators, but the data were sparse because this information was not included until somewhat recently. We plan to test our predictions on future generators to determine the broader applicability and to evaluate the clinical impact once more multiyear records are available.

DISCLOSURE

Mark Hyun served as a technical consultant to Astellas regarding the Lexiscan product. No other potential conflict of interest relevant to this article was reported.

ACKNOWLEDGMENTS

We acknowledge Jeffrey Metcalf, CNMT, for his assistance in collecting the data, Dr. Adrian Nunn of Bracco Imaging for information on ^{82}Rb generators, and Dr. Dan Berman, FACC, for contributing to the original research concept.

KEY POINTS

QUESTION: Can an ^{82}Rb generator bolus duration be predicted as a function of activity eluted and the generator age?

PERTINENT FINDINGS: For a particular generator model, the activity output rate was fitted with a growth-saturation curve and the times to achieve certain eluted activities were fitted as a function of generator age using an exponential curve and symmetric bands to capture 95% of the data points.

IMPLICATIONS FOR PATIENT CARE: Utilizing these calculations allows patients to be rescheduled if their predicted injection time given the prescribed ^{82}Rb activity and generator age would exceed the preset bolus duration limit.

REFERENCES

1. Dilsizian V. Transition from SPECT to PET myocardial perfusion imaging: a desirable change in nuclear cardiology to approach perfection. *J Nucl Cardiol.* 2016;23:337–338.
2. Bateman TM, Dilsizian V, Beanlands R, DePuey E, Heller G, Wolinsky D. American Society of Nuclear Cardiology and Society of Nuclear Medicine and Molecular Imaging joint position statement on the clinical indications for myocardial perfusion PET. *J Nucl Med.* 2016;57:1654–1656.
3. Murthy VL, Bateman TM, Beanlands RS, et al. Clinical quantification of myocardial blood flow using PET: joint position paper of the SNMMI Cardiovascular Council and the ASNC. *J Nucl Med.* 2018;59:273–293.
4. Nagamachi S, Czernin J, Kim AS, et al. Reproducibility of measurements of regional resting and hyperemic myocardial blood flow assessed with PET. *J Nucl Med.* 1996;37:1626–1631.
5. Case JA, deKemp RA, Slomka PJ, Smith MF, Heller GV, Cerqueira MD. Status of cardiovascular PET radiation exposure and strategies for reduction: an information statement from the Cardiovascular PET Task Force. *J Nucl Cardiol.* 2017;24:1427–1439.
6. Bateman TM, Heller GV, Beanlands R, et al. Practical guide for interpreting and reporting cardiac PET measurements of myocardial blood flow: an information statement from the American Society of Nuclear Cardiology, and the Society of Nuclear Medicine and Molecular Imaging. *J Nucl Med.* 2021;62:1599–1615.
7. Crackett RV. ^{82}Sr production from metallic Rb targets and development of an ^{82}Rb generator. *Appl Radiat Isot.* 1993;44:917–922.